ORIGINAL ARTICLE

Microtubule-dependent processes precede pathological calcium influx in excitotoxin-induced axon degeneration

Nan Tian[1] (iD), Kelsey A. Hanson[1] (iD), Alison J. Canty (iD), James C. Vickers (iD) and Anna E. King (iD)

Wicking Dementia Research and Education Centre, University of Tasmania, Hobart, Tasmania, Australia

Abstract

Axon degeneration and axonal loss is a feature of neurodegenerative disease and injury and occurs via programmed pathways that are distinct from cell death pathways. While the pathways of axonal loss following axon severing are well described, less is known about axonal loss following other neurodegenerative insults. Here we use primary mouse cortical neuron cultures grown in compartmentalized chambers to investigate the role of calcium in the degeneration of axons that occurs following a somal insult by the excitotoxin kainic acid. Calcium influx has been implicated in both excitotoxicity and axon degeneration mechanisms, however the link between a somal insult and axonal calcium increase is unclear. Live imaging of axons demonstrated that pharmacologically preventing intracellular calcium increases through the endoplasmic reticulum or mitochondria significantly ($p < 0.05$) reduced axon degeneration. Live calcium-imaging with the Ca^{2+} indicator Fluo-4 demonstrated that kainic acid exposure to the soma resulted in a rapid, and transient, increase in calcium in the axon, which occured even at low kainic acid concentrations that do not cause axon degeneration within 24 h. However, this calcium transient was followed by a gradual increase in axonal calcium, which was associated with axonal loss. Furthermore, treatment with a range of doses of the microtubule stabilizing drug taxol, which protects against axon fragmentation in this model, prevented this gradual calcium increase, suggesting that the intra-axonal calcium changes are downstream of microtubule associated events. Biochemical analysis of taxol treated neurons demonstrated a shift in microtubule post-translational modifications, with a significant ($p < 0.05$) increase in acetylated tubulin and a significant ($p < 0.05$) decrease in tyrosinated tubulin, suggestive of a more stable microtubule pool. Together our results suggest that axonal degeneration following excitotoxicity is dependent on an increase in axonal calcium, which is downstream of a microtubule-dependent event.

Keywords: axon degeneration, calcium signalling, excitotoxin, microtubule.

J. Neurochem. (2019) https://doi.org/10.1111/jnc.14909

Axon degeneration occurs in a number of neurodegenerative diseases and it is now clear that axons can regulate their own localized or global degeneration independently of cellular apoptosis or other known cell death pathways (reviewed in Hilliard 2009; Wang *et al.*, 2012). While mechanisms of degeneration following axon severing (Wallerian degeneration) have been well described, less is known about axon degeneration following pathogenic insults, such as excitotoxicity. We have previously shown that excitotoxic stimulation of the cell soma with kainic acid induces axon degeneration in the untreated axon, characterized by axon beading and fragmentation as well as caspase activation

ORIGINAL ARTICLE

(King *et al.,* 2013). Furthermore, microtubule-stabilizing drugs inhibit axon fragmentation implicating microtubule depolymerization in excitotoxin-induced axon fragmentation (King *et al.,* 2013). However, the key events that lead to microtubule destabilization in axons following excitotoxic insult to the soma and dendrites are currently unclear.

One of the key effects of an excitotoxic insult is an increase in intracellular calcium, chiefly through NMDA receptors, calcium permeable α-amino-3-hydroxy-5-methyl-4-isoxazolepropionic acid (AMPA) receptors or release from internal stores (Tymianski and Tator, 1996, Pellegrini-Giampietro *et al.,* 1997, Ruiz *et al.,* 2009; reviewed in Szydlowska and Tymianski, 2010). Importantly, calcium alterations have been shown to be the mediators of the effects of excitotoxicity on the neuron (Cheng *et al.,* 1999, reviewed in Arundine and Tymianski, 2004). However, the soma and dendrites, where the majority of glutamate receptors are localized, are spatially separated from the axon, suggesting that direct excitotoxin-induced calcium influx at the soma and dendrites may be unlikely to be the cause of axon degeneration. In spite of this, axonal calcium changes are potentially involved in excitotoxin-induced axon degeneration, and calcium has been demonstrated to play a role in described forms of axon degeneration including Wallerian degeneration and developmental axon pruning.

Following severing of an axon, there is a localized increase of calcium in the proximal damaged segments (Vargas *et al.,* 2015), which early studies have shown is important for resealing the cut ends of the axon (Yawo and Kuno, 1985). This early calcium flux is followed by a lag phase and a second global calcium increase throughout the severed end of the axon (Adalbert *et al.,* 2012; Vargas *et al.,* 2015), which is prevented by expression of the Wallerian degeneration protective protein Wlds (Adalbert *et al.,* 2012). Inhibition of this second calcium increase delays axon fragmentation. Similarly, developmental axon pruning and axonal stretch injury have also been linked to calcium changes in the axon (Staal *et al.,* 2010; Yang *et al.,* 2013).

The source of calcium involved in signalling cascades in axon degeneration is not well described. In the axon, increases in axonal calcium could arise from a number of compartments including release from internal stores or influx from the extracellular environment. The endoplasmic reticulum (ER) plays an important role in the regulation of calcium as a second messenger in the cell and, although not well characterized, is present within axons, usually as smooth ER (reviewed in Luarte *et al.,* 2018). The ER releases calcium through two main routes, the ryanodine receptors, which are stimulated by increases in intracellular calcium (calcium induced calcium release or calcium-induced calcium release) and the IP3 receptors, which are stimulated by Phospholipase C (reviewed in Mattson *et al.,* 2000). Axonal ER is tightly coupled to mitochondria (Wu at al., 2017), another intracellular source of calcium. Mitochondrial calcium uptake and export through the mitochondrial uniporter and the mitochondrial sodium/calcium exchanger are coupled to altered energy production (reviewed in Arduino and Perocchi, 2018). However, a key mitochondrial calcium exporter in terms of calcium overload and pathological conditions is the permeability transition pore (PTP). Blocking ER calcium release and PTP opening have been shown to be protective against Wallerian degeneration-induced axon fragmentation (Villegas *et al.,* 2014). Influx of calcium can also occur from the extracellular space through voltage-gated calcium channels, transient receptor potential channels or reverse operation of the sodium/calcium exchanger (Szydlowska and Tymianski, 2010). The subtype-specific expression of voltage-gated calcium channels on axon shafts and branches is beginning to be described. Chelating extracellular calcium or blocking voltage-gated calcium channels have both been shown to delay axon fragmentation following axon severing (Knoferle *et al.,* 2010; Mishra *et al.,* 2013).

In this study, we have used a cell culture model, involving the growth of primary murine cortical neurons in compartmentalized microfluidic chambers, and live cell imaging to investigate calcium signalling in the untreated axon following excitotoxic kainic acid stimulation of the somatodendritic compartment. We have investigated the role of calcium sources in signalling, as well as the role of calcium in subsequent axon degeneration. Furthermore, we investigated whether axonal calcium alterations are up- or down-stream of axonal microtubule changes.

Material and methods

Animals used in study

In this study, mice were bred at the Central Farm Facility (University of Tasmania). Here 69 time-mated C57BL/6J mice (217 embryos) were used to derive cells for primary culture. Each independent culture preparation was derived from the combined embryos of a single time-mated mouse. Tissue from these mice contributed to other projects. All use of animals was approved by the animal ethics committee of the University of Tasmania (A0015121 and A17530) and performed in accordance with the Australian Code of Practice for the Care and Use of Animals for Scientific Purposes developed by the National Health and Medical Research Council. Randomization and sample calculations were not carried out. This study was not pre-registered.

Primary cell culture in microfluidic chambers

Primary mouse cortical cell culture was performed as we have described previously (Hosie *et al.,* 2012; King *et al.,* 2013). Cortical neurons were prepared from 217 embryonic day 15.5 embryos of either sex. The pregnant females (the dams) were asphyxated using CO_2, which is a method of humane killing recommended by ANZCCART (Australian and New Zealand Council for the Care of Animals in Research and Teaching) and embryos were removed and decapitated. Cortical tissue was dissected from mouse embryos and

dissociated using 0.0125% trypsin (5 min at 37°C). Tissue was mechanically triturated in cell plating media consisting of Neurobasal media (Gibco, Rockville, MD, USA, catalog #21103049), 2% B27 supplement (Gibco, catalog #17504044), 0.5 mM glutamine, 25 mM glutamate, 10% fetal calf serum (Gibco, catalog #10099141) and 1% antibiotic/antimycotic (Gibco) using a 1ml pipette. Cell viability and density was assessed using a trypan blue exclusion assay. Cells (1.2×10^5 per chamber) were plated into the somatodendritic compartment of a 450 μm microfluidic chamber (Xona, Durham, NC, USA, catalog #SND450) coated with poly-L-lysine substrate (0.001%; Sigma, St Louis, MO, USA, catalog #P4707) or directly onto 13 mm poly-L-lysine coated coverslips (30 000 cell per coverslip). Cells were allowed to adhere to the substrate for 30 min prior to filling chambers with cell plating media. The following day, media was changed to cell maintenance media consisting of plating media without the fetal calf serum and glutamate. Cells were grown in 5% CO_2 at 37°C.

Calcium imaging of cultured cortical neurons

For cytosolic calcium measurements, the membrane permeable fluorescent Ca^{2+} indicator Fluo-4 Direct (Invitrogen, Carlsbad, CA, USA, catalog #F10471) was used. Cortical neurons of relative maturity (9 DIV) were loaded with 2× Fluo-4 Direct stock solution to the cell culture media and incubated for 1 h in a 5% CO_2-humidified incubator at 37°C. Time-lapse imaging was performed using a Nikon TiE motorized inverted microscope (Nikon, Tokyo, Japan). For short (2 min) calcium imaging recording, cell culture media was replaced by Hanks' Balanced Salt solution (HBSS; Gibco), and images were captured either every 400 msec with a 20× air objective lens or every 1 s with a 40× air objective. For longer term (60/90 min) calcium imaging recording, cell maintenance media was used for imaging and images were captured every 2 min using a 40× air objective lens. After 1-min of baseline recording, kainic acid (Sigma, catalog #K0250) solution was added to the somatodendritic compartment by pipetting. Calcium activity was measured as the average pixel intensity (F) in a randomly selected region of the axonal compartment and identical regions (100 × 100 μm) were analysed in all experiments. Graphs representing calcium changes were calculated as relative fluorescence changes compared to fluorescence intensity at the beginning (F0) according to the following formula: (F-F0)/F0. Signal intensities were determined using Fiji software (Plot Z-axis profile, NIH ImageJ; RRID:SCR_003070, Madison, WI, USA). To plot changes of calcium intensity over 60–90 min, the average intensity values from images collected every 2 min were used. For quantification of Ca^{2+} peak intensity, the time point showing the highest signal intensity after kainic acid treatment was used. Data were collected from three arbitrary fields per recording, from a total of three or four independent cell cultures.

Pharmacological manipulation

Unless otherwise indicated, cells were treated with 50 μM kainic acid or vehicle control at DIV 9 corresponding to a time of dense axonal growth in the axon chamber. For dose-dependent experiments, 100 μM, 50 μM, 25 μM, 12.5 μM or 5 μM kainic acid was added to the cells as indicated.

For intracellular calcium chelation and calcium channel inhibition, 6 μM 1,2-bis(o-aminophenoxy)ethane-N,N,N',N'-tetraacetic acid (BAPTA)-AM (Invitrogen, catalog #B6769), 10 μM 2-aminoethoxydiphenyl borate (2APB, Sigma, catalog #D9754), 10 μM Dantrolene sodium salt (Sigma, catalog #D9175) or 10 μM Cyclosporin A (Sigma, catalog #30024) was added to the axonal chamber along with Fluo-4, 1 h before imaging. For extracellular calcium chelation, 1 mM EGTA (Sigma, catalog # E3889) was added to the imaging medium, as indicated.

To block the action potential, 1 μM Tetrodotoxin (Sigma, catalog #T8024) was added to the axonal chamber along with Fluo-4, 1 h before imaging. To stabilize microtubules, 1000, 100 or 10 ng/mL Taxol (Sigma, catalog #T7402) was added to the axonal chamber along with Fluo-4, 1 h before imaging.

ELISA analysis

Cortical neurons were grown in microfluidic chambers for 9 days *in vitro* prior to treatment with10 ng/mL taxol for 2 h. Plating media was removed from cortical neurons, and cultures were rinsed with HBSS. Cells were harvested with RIPA buffer with protease inhibitors (Roche Molecular Biochemicals, Indianapolis, IN, USA, catalog #4693159001) and phosphatase inhibitors (A.G. Scientific, San Diego, CA, USA, catalog #P-1517). Samples were centrifuged at 11 400 g for 1 min and pellets were discarded. Samples were diluted at 1 : 300 in 50 μL carbonate/carbonate coating buffer (Abcam, Melbourne, Australia, catalog #ab210899), added to a 96-well plate and incubated overnight at 4°C. For the standard curve, protein samples were serially diluted at 1 : 100, 1 : 200, 1 : 400, and 1 : 800. A blank and no primary control were incubated to correct for ELISA results. Plates were washed with washing buffer (0.01 M phosphate-buffered saline with 0.05% tween-20) prior to blocking with blocking buffer (0.01 M phosphate-buffered saline with 5% fetal bovine serum) and incubated at 37°C for 30 min. Plates were washed prior to incubation with detecting antibodies (acetylated tubulin 1 : 500, mouse; Sigma, catalog #T7451; tyrosinated tubulin 1 : 500 rabbit; Millipore Corporation, Bedford, MA, USA, catalog #ABT171) diluted in blocking buffer for 1 h at 20°C. Plates were washed and incubated with species-specific HRP secondary antibody (Dako, Carpinteria, CA, USA) diluted in blocking buffer at 1 : 2000 and incubated at 20°C for 45 min. Plates were washed and incubated with 20°C tetramethylbenzidine substrate (Thermo Scientific, Scoresby, Australia, Lot # SA2328991) for 15 min. The reaction was stopped by 0.1 M H_2SO_4. Plates was read using plate reader at 450 nm. Cells were pooled from two to three chambers per treatment from five separate cultures.

Axon degeneration

Live imaging of axons was acquired on a Nikon TiE motorized inverted microscope, with chambers maintained at 37°C. For quantitation of axon degeneration, images were acquired of the axonal compartment prior to cell treatment and from an identical area at 18 h after treatment. The axon degeneration of primary cortical neurons was quantitated by an observer blinded to experimental settings during axon counting. Five arbitrarily chosen images for each coverslip, total 6–8 coverslips, collected from three to four independent cell cultures were taken for quantification. Beaded and/or fragmented axons were scored as evidence of degeneration. Numbers of degenerated axons were normalized to pre-treated counts for each image. Degenerated axons were divided by the total number of axons for the percentage degeneration.

Statistics

All statistical analysis and graphs were prepared in GraphPad Prism (7.0). Prior to data analysis, outliers were designated as data points outside the 95% confidence interval and would be excluded from the data analysis. Data are given as mean ± SEM. Statistical differences were calculated using one-way ANOVA followed by Dunnett's multiple comparisons test; significance was considered at $p < 0.05$. The normality of data was not evaluated. No animals were specifically excluded. Cultures were excluded if they did not grow through the microfluidic channels, or if there was evidence of neurodegeneration (identified by cell loss, beaded and fragmented neurites) in control cultures.

Results

Somal kainic acid exposure results in a rapid calcium transient followed by a gradual increase in calcium in the untreated axon

In order to determine the effect of somatodendritic kainic acid exposure on axonal calcium, we performed live imaging with the fluorescent calcium indicator Fluo-4 which provided a sufficient dynamic range to observe rapid and discrete calcium alterations in a spatio-temporal manner (Fig. 1a). In untreated cultures, occasional calcium transients were seen in individual axons (Fig. 1b). To induce excitotoxicity, we applied 50 μM kainic acid, a concentration we have previously shown to induce moderate axon degeneration (King *et al.,* 2013), to the somatodendritic compartment of the chamber, and imaged calcium transients in the axonal compartment. Exposure to kainic acid induced a rapid (within 5 s) increase in calcium across the axonal compartment. These calcium transients reached the highest amplitude and returned to baseline within 20 s (Fig. 1a and c). Qualitative analysis of these transients demonstrated that calcium increases were present in the majority of axons. The rapid calcium peak was followed by a gradual calcium increase in the untreated axons, which reached a steady phase about 60 min following kainic acid application (Fig. 1d and f). A weak calcium increase was observed in the sham control during the lag phase, potentially due to the stress of the cells during recording. Interestingly, the calcium amplification in the gradual phase was higher than the first peak (Fig. 1e) and was accompanied by the focal swelling of axons (Fig. 1f).

Relationship between kainic acid–induced axon degeneration and intra-axonal calcium increase

We next examined the dose range of kainic acid that resulted in axon degeneration and calcium increase. To examine axon degeneration, a range of concentrations from 5 to 100 μM of kainic acid were applied to the somatodendritic compartment and the amount of axon degeneration examined 18 h later.

Qualitatively, 100 μM kainic acid induced extensive axon fragmentation, whereas 50 μM and 25 μM kainic acid induced degrees of axon beading with partial fragmentation (Fig. 2a). Quantitative analysis of axon degeneration demonstrated that while significant axon degeneration (beading and fragmentation) was present from 25 μM to 100 μM kainic acid, at concentrations below 25 μM (12.5 μM, 5 μM) kainic acid, no significant ($p < 0.05$) axon degeneration was present compared with the control group (Fig. 2a and b).

To determine the relationship between kainic acid dose and calcium influx, we imaged axonal calcium influx over a range of concentrations of kainic acid from 5 to 100 μM. For the fast phase of calcium increase, 5 μM kainic acid was not sufficient to induce a calcium influx in the axons, however concentrations of kainic acid at or above 12.5 μM induced a significant increase in axonal calcium. The calcium influx in the axon was not dependent on the concentration of kainic acid, with conentrations from 12.5 to 100 μM inducing similar calcium amplitudes, suggesting a threshold response. These data suggest that somatodendritic exposure to kainic acid induces an influx of cytoplasmic calcium along the untreated axon that is an all-or-nothing response (Fig. 2c). Since 12.5 μM kainic acid induced a rapid calcium transient but did not result in axon degeneration, this implies that the initial kainic acid induced calcium transient is unlikely to be sufficient to cause axon degeneration. Concentrations of kainic acid at or above 25 μM induced a significant increase in axonal calcium as compared to the vehicle control (Fig. 2d). The sustained phase of calcium increase in axons showed a similar dose related pattern with axon degeneration, which suggests that the gradual axonal calcium increase plays a more important role in axon degeneration.

Regulation of the two phases of calcium increase

To assess whether the calcium increases are coupled with action potentials, 1 μM of tetrodotoxin was added to the axonal compartment while the somal compartment was exposed to 50 μM of kainic acid. The fast calcium rise was completely blocked by addition of tetrodotoxin 1 h prior to kainic acid treatment (Fig. 3a and c), and the gradual calcium increase was attenuated during 90 min of kainic acid exposure (Fig. 3b d and e), suggesting the action potential plays a role in triggering calcium influx and that the gradual calcium increase may be partially dependent on the fast calcium increase.

We have previously implicated microtubule-dependent processes in axon degeneration, and shown that microtubule stabilization with taxol in the axonal compartment inhibits kainic acid induced axon degeneration (King *et al.,* 2013). To determine the relationship between microtubule destabilization and calcium influx, we added taxol to the axonal compartment 1 h prior to kainic acid treatment. The fast calcium rise was not affected by pre-treatment with taxol (Fig. 3a and c), however, the gradual calcium increase was significantly reduced compared to the vehicle control (Fig. 3b, d and e) and was not significantly different from untreated cultures (see Fig. 1d). To further determine the
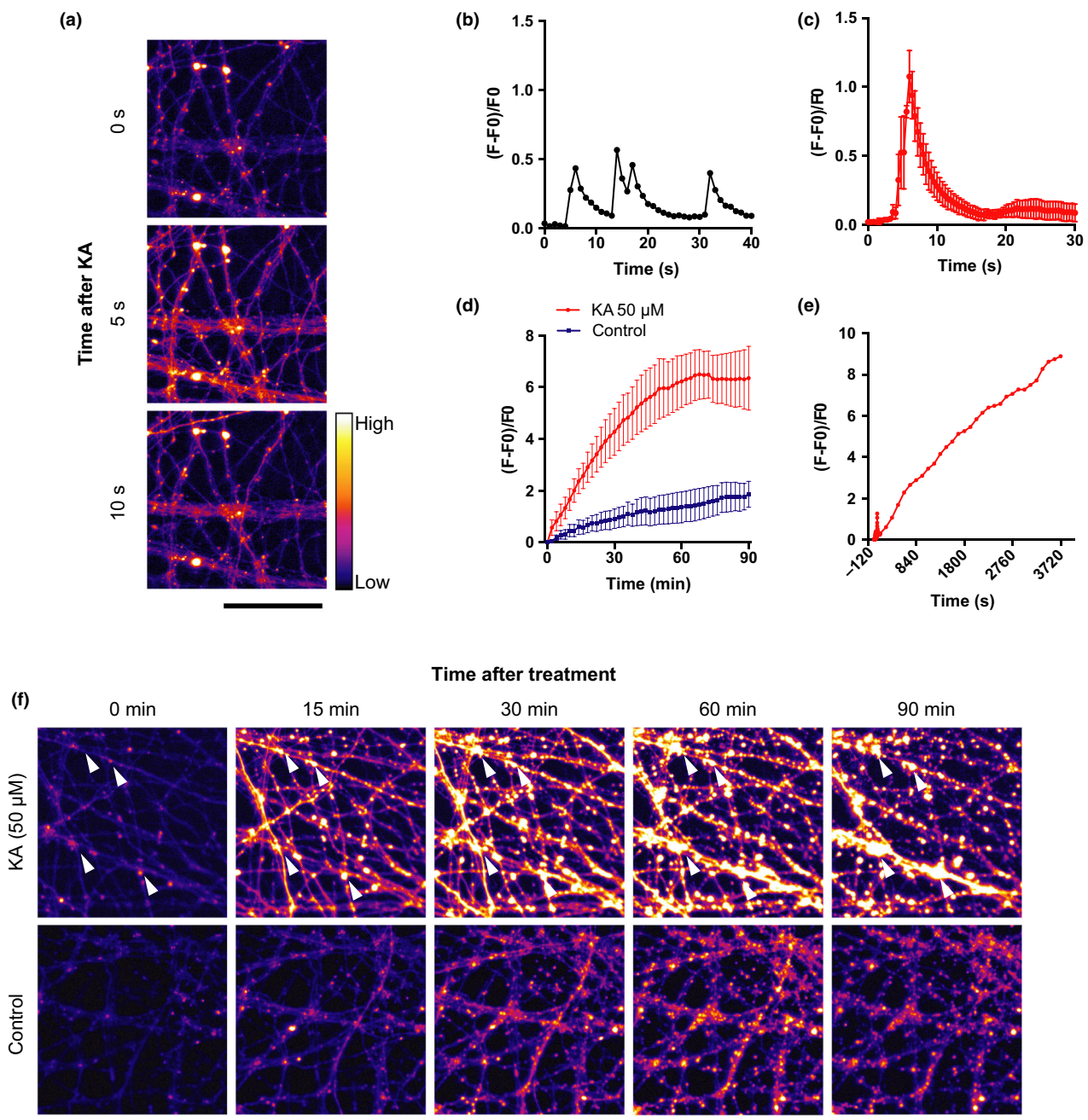
Fig. 1 KA induced a rapid intra-axonal calcium peak followed by a long-term gradual calcium increase. (a) Axons of cultured cortical neurons loaded with calcium indicator Fluo-4 before (0 s) and after somal KA treatment (5 and 10 s). The arbitrary colour scale at the right indicates relative levels of calcium. Scale bar, 50 µm. (b) Example of spontaneous axonal calcium transients before KA treatment. (c) Plot of relative calcium intensity changes in the axons after KA treatment for 30 s. Mean ± SEM; $n = 3$ independent cell culture preparations. (d) Plot of relative calcium intensity changes in the axons during the gradual phase after KA treatment. Mean ± SEM; $n = 3$ independent cell culture preparations. (e) Representative data showing the combination of the fast phase and gradual phase of axonal calcium increase after KA treatment. (f) Gradual axonal calcium alteration after KA or vehicle treatment for 90 min. Arrows indicate the high calcium activity spots.

concentration range that taxol is able to prevent the gradual calcium increase after kainic acid treatment, the effects of 100 and 10 ng/mL axonal taxol were tested by calcium imaging. Both 100 and 10 ng/mL axonal taxol reduced the gradual calcium increase significantly, as compared to vehicle control (Fig. 3f and g). These results indicate that
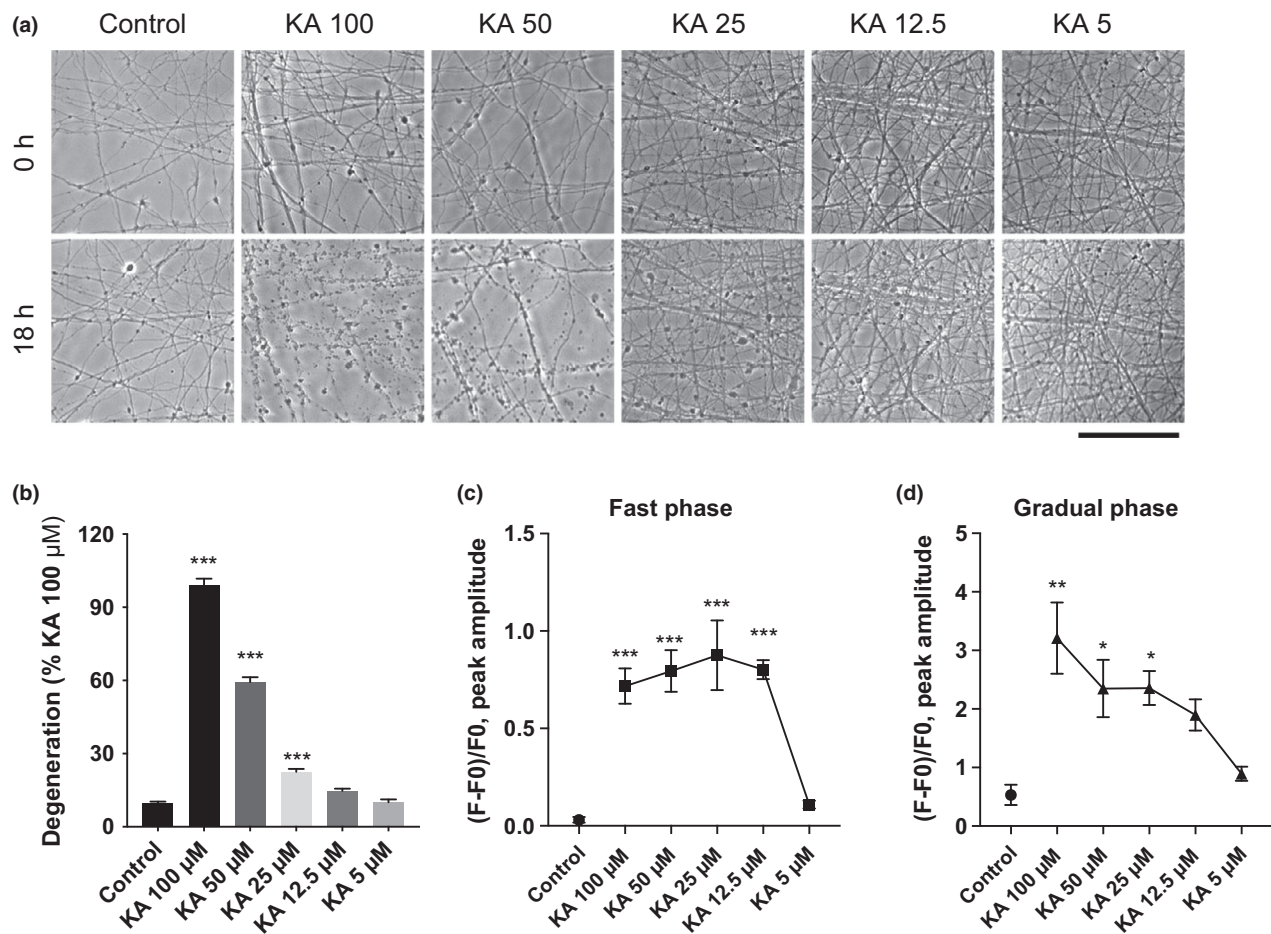
Fig. 2 KA induced axon degeneration and axonal calcium increase. (a) Phase images of axons acquired before (0 h) and after different dose of KA treatment (18 h). Scale bar, 50 μm. (b) Percentage of axon degeneration was calculated after different doses of KA treatment. Mean ± SEM; $n = 30$ analysed images; one-way ANOVA followed by Dunnett's multiple comparisons test; ***$p < 0.001$. (c) Quantification of relative calcium peak intensity of initial calcium peak after kainic acid treatment. Mean ± SEM; $n = 12$ analysed fields; one-way ANOVA followed by Dunnett's multiple comparisons test; ***$p < 0.001$. (d) Quantification of relative calcium intensity at 60 min after KA treatment. Mean ± SEM; $n = 9$ analysed fields; one-way ANOVA followed by Dunnett's multiple comparisons test; *$p < 0.05$, **$p < 0.01$.

microtubule-associated events play a role in the gradual increase of calcium in the axon, but not in the fast phase of calcium influx.

To further investigate microtubule alterations that may be responsible for this effect on the gradual calcium influx, we next investigated changes in microtubule post-translational modifications following taxol application to cortical neurons growing on coverslips. ELISA analysis demonstrated that 2 h after 10 ng/mL taxol treatment, acetylated tubulin levels were significantly up-regulated and tyrosinated tubulin levels were down-regulated ($p < 0.05$). These data suggest that taxol pre-treatment increases the stabilization of neuronal microtubules (Fig. 3h and i).

Chelating intra-axonal calcium prevents axon degeneration
To investigate the role of intracellular and extracellular calcium in axon degeneration, we used EGTA and the cell

permeant BAPTA-AM to chelate extracellular and intracellular calcium, respectively. While both calcium chelators caused a significant ($p < 0.05$) decrease in both the fast (Fig. 4a and b) and the gradual calcium increases as compared to the vehicle control (Fig. 4c–e), axon degeneration was only significantly altered by the addition of BAPTA-AM, with no significant ($p < 0.05$) effect of EGTA. We therefore investigated the source of intracellular calcium that results in axonal calcium increases and axon degeneration.

Somatodendritic kainic acid exposure induces calcium release from axonal ER and mitochondria
In axons, most calcium is stored in the ER or mitochondria. To clarify the role of intracellular calcium stores in kainic acid induced axonal calcium transients, the fast calcium signal was examined in the presence of specific calcium
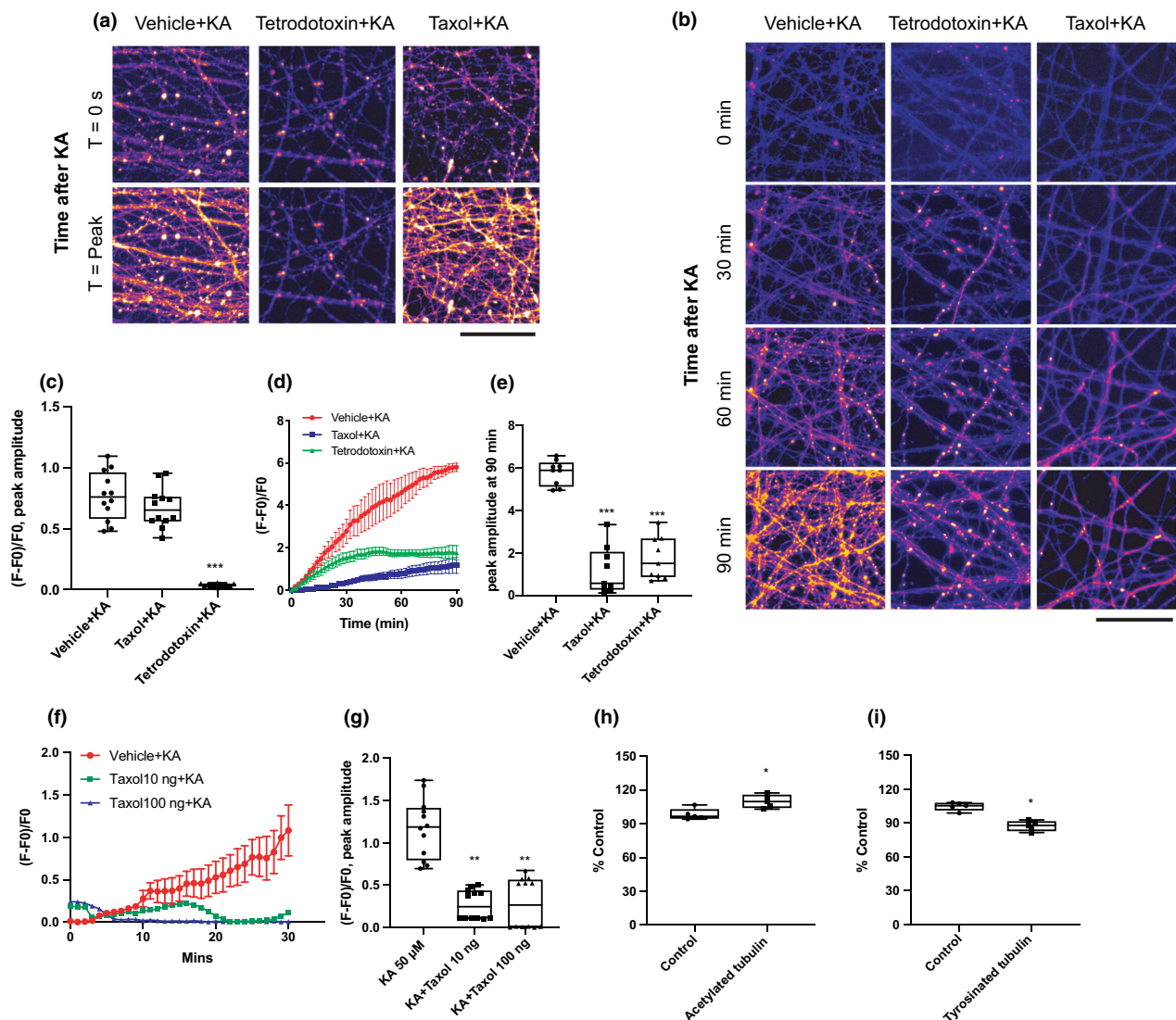
Fig. 3 The regulation of fast phase and the gradual phase of axonal calcium increase. (a) The initial calcium peak is prevented by tetrodotoxin but not Taxol. Axons of cortical neurons loaded with Fluo-4 before (T = 0 s) and after somal KA treatment (T = peak). Scale bar, 50 μm. (b) The gradual phase of axonal calcium changes with pre-treatment with tetrodotoxin and taxol. Axons of cortical neurons loaded with Fluo-4 before (0 min) and after somal KA treatment (30 min, 60 min, 90 min). Scale bar, 50 μm. (c) Quantification of initial calcium peak intensity. Mean ± SEM; $n = 12$ analysed fields; one-way ANOVA followed by Dunnett's multiple comparisons test; ***$p < 0.001$. (d) Plot of relative calcium intensity changes in the axons during the gradual phase after KA treatment. Mean ± SEM; $n = 9$ analysed fields. (e) Quantification of relative calcium intensity at 90 min after KA treatment. Mean ± SEM; $n = 9$ analysed fields; one-way ANOVA followed by Dunnett's multiple comparisons test; ***$p < 0.001$. (f) Representative plots of gradual phase axonal calcium changes with pre-treatment with different dose of taxol. Mean ± SEM; $n = 3$ analysed fields. (g) Quantification of relative calcium intensity at 30 min after KA treatment. Mean ± SEM; $n = 12$ analysed fields; one-way ANOVA followed by Dunnett's multiple comparisons test; **$p < 0.01$. (h and i) ELISA analyse of acetylated and tyrosinated tubulin levels at 2 h after taxol (10 ng/mL) treatment. Mean ± SEM; $n = 5$ independent cell culture preparations; one-way ANOVA followed by Dunnett's multiple comparisons test; *$p < 0.05$.

channel blockers applied to the axonal compartment. Ryanodine and IP3 receptors were blocked using dantrolene or 2APB, respectively, to examine the contribution of the ER calcium channels. To examine mitochondrial calcium channel, the mitochondrial permeability transition pore (MPTP) was blocked using Cyclosporin A. While 2APB had little effect on the fast calcium transient, both dantrolene and Cyclosporin A significantly reduced the amount of cytoplasmic calcium in the axon (Fig. 5a and b). These data suggest that the fast calcium transient is dependent on a combined release of calcium from ER and mitochondrial stores.
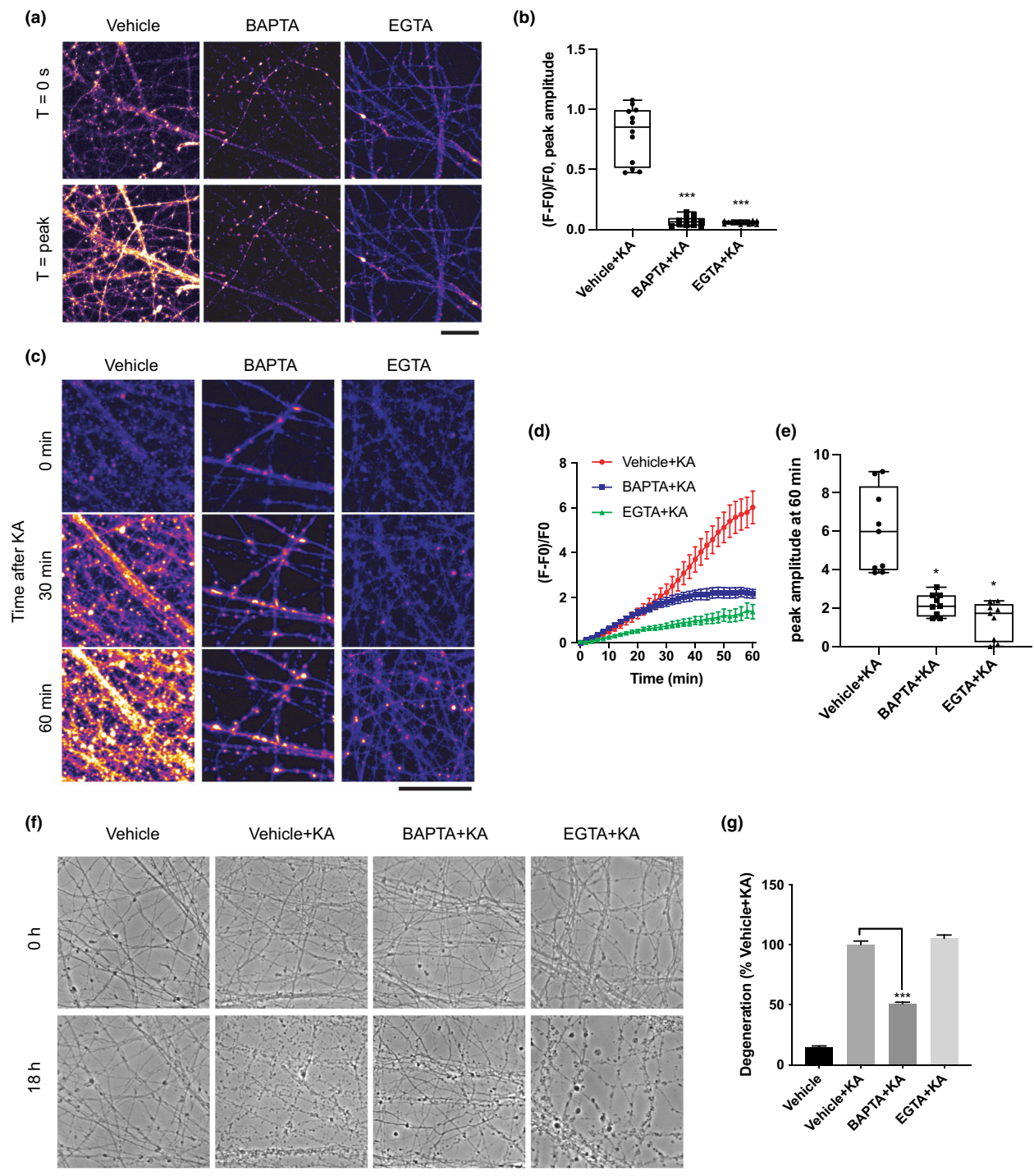
Fig. 4 The intra-axonal calcium store is the main source of somal KA induced axon degeneration. (a) Treatment with either EGTA or BAPTA-AM prevents axonal rapid calcium peak induced by KA. Scale bar, 50 mm. (b) Quantification of relative calcium peak intensity. Mean ± SEM; n = 18 analysed fields; one-way ANOVA followed by Dunnett's multiple comparisons test; ***p < 0.001. (c) The gradual phase of axonal calcium changes with pre-treatment with BAPTA and EGTA. Axons of cortical neurons loaded with Fluo-4 before (0 min) and after somal KA treatment (30 min, 60 min). Scale bar, 50 mm. (d) Plot of relative calcium intensity changes in the axons during the gradual phase after KA treatment. Mean ± SEM; n = 9 analysed fields. (e) Quantification of relative calcium intensity at 60 min after KA treatment. Mean ± SEM; n = 9 analysed fields; one-way ANOVA followed by Dunnett's multiple comparisons test; *p < 0.05. (f) Phase images of axons acquired before (0 h) and after different doses of KA treatment (18 h). Scale bar, 50 mm. (g) Percentage of axon degeneration normalized to Vehicle + KA. Mean ± SEM; n = 40 analysed images; one-way ANOVA followed by Dunnett's multiple comparisons test; ***p < 0.001.

We then asked whether the ER and mitochondrial calcium stores also contribute to the gradual axonal calcium increase after somatodendritic kainic acid exposure. Dantrolene and Cyclosporin A, which reduced the fast calcium increase, also significantly reduced the gradual phase calcium increase (Fig. 5c and d). The quantification of the calcium peak intensity of gradual phase calcium signals showed a drastic decrease in the presence of dantrolene or Cyclosporin A in the axonal compartment (Fig. 5e). These data suggest that calcium released from axonal ER and mitochondria contribute to kainic acid-induced axonal calcium increase.

Inhibition of calcium release from intra–axonal stores prevents axon degeneration

We next asked whether blocking intra-axonal calcium release could prevent axon degeneration induced by somatodendritic kainic acid exposure. Axons were pre-incubated for 1 h with Dantrolene and Cyclosporin A, respectively. Axon degeneration was quantitated at 18 h post-kainic acid treatment. Axon protection was observed when axons were pre-incubated with either dantrolene or Cyclosporin A. These results suggest that the intra-axonal calcium release from ER and mitochondria contributes to axon degeneration induced by somatodendritic kainic acid exposure (Fig. 5f and g).

Discussion

Axon degeneration is a key feature of a number of neurodegenerative diseases including amyotrophic lateral sclerosis, Alzheimer's disease and Parkinson's disease (reviewed in Vickers *et al.,* 2009). Although the cause of axon degeneration in these diseases is unclear, excitotoxicity is a key pathological mechanism implicated in disease progression and a potential cause of axonal loss (reviewed in King *et al.,* 2016; Wang and Reddy, 2017). Disease-associated excitotoxicity can be mediated through NMDA or AMPA/kainate receptors and the specific source of excitotoxicity may differ between diseases (e.g Heath and Shaw 2002; Wang and Reddy, 2017). We have previously shown that exposure of the somatodendritic compartment of cultured cortical neurons to the excitotoxin kainic acid, an AMPA/kainate receptor agonist, induces degeneration in the untreated axon (King *et al.* 2013). Furthermore, kainic acid induced axon degeneration was inhibited by application of the microtubule stabilizing drug taxol to the axon (King *et al.* 2013). This project sought to investigate the role of axonal calcium signalling, implicated in excitotoxin-induced cell death (Arundine and Tymianski, 2003), and the relationship to microtubule changes, in downstream axon degeneration pathways. We hypothesized that calcium signalling from the soma to the axon could be involved in initiating a sequence of changes resulting in axon fragmentation. We show that an initial somatodendritic excitotoxic insult with kainic acid results in a rapid calcium influx in the axonal compartment, which occurs even at low concentrations of kainic acid that do not induce axon degeneration within 18 h. The initial rapid calcium transient is followed by a gradual calcium rise in the axon, which is dose dependent. Application of taxol to the axonal compartment, which we have previously shown to prevent axon fragmentation, did not affect the initial calcium transient, but prevented the gradual calcium increase. Chelation of intracellular calcium prevented axon degeneration and was linked to release of calcium from endoplasmic reticulum (through ryanodine receptors) and through the mitochondrial permeability transition pore. These data suggest that excitotoxicity applied to the somatodendritic compartment induces a rapid, but non-pathologic calcium transient and that axon degeneration is dependent on a second gradual increase in calcium from internal stores, which is downstream from microtubule-associated processes.

Somatodendritic exposure to kainic acid induces an axonal calcium transient followed by a gradual rise in calcium

Our data show that application of kainic acid induced a rapid calcium transient in the axonal compartment, which was tetrodotoxin dependant and appeared to progress in an "all or nothing" fashion at concentrations tested above 5 μM. This suggests that the initial calcium transient is linked to the action potential. A number of pieces of evidence suggest that this initial calcium transient is not sufficient to induce axonal degeneration. Firstly, this initial calcium transient occurred even at relatively low concentrations of kainic acid (12.5 μM); concentrations that did not result in axonal fragmentation over the time-course examined. Secondly, the initial calcium transient was still present in the presence of taxol, which we have previously shown protects against axon fragmentation.

The initial calcium transient was followed by a more gradual calcium rise which peaked at about 60 min following exposure to kainic acid. The second calcium increase was dose-dependent, and like the first calcium peak was blocked by tetrodotoxin, implicating sodium channels and the action potential. However, unlike the first peak, the second calcium increase was blocked in the presence of taxol, suggesting mechanistic differences to the first calcium peak and that this calcium increase plays a role in the induction of axon degeneration processes. Our data are in line with previous studies that have investigated calcium alterations in other forms of axonal injury, particularly Wallerian degeneration. Vargus *et al.* (2015) investigated calcium alterations in zebrafish sensory axons undergoing Wallerian degeneration and demonstrated an initial localized benign calcium influx, which was followed by a terminal calcium rise prior to fragmentation. Similar effects have been reported in cultured neurons following transection (Villegas *et al.,* 2014), where expression of the wlds protein did not affect initial calcium increases but prevented the later calcium rise and downstream degeneration (Adalbert *et al.,* 2012). Furthermore,
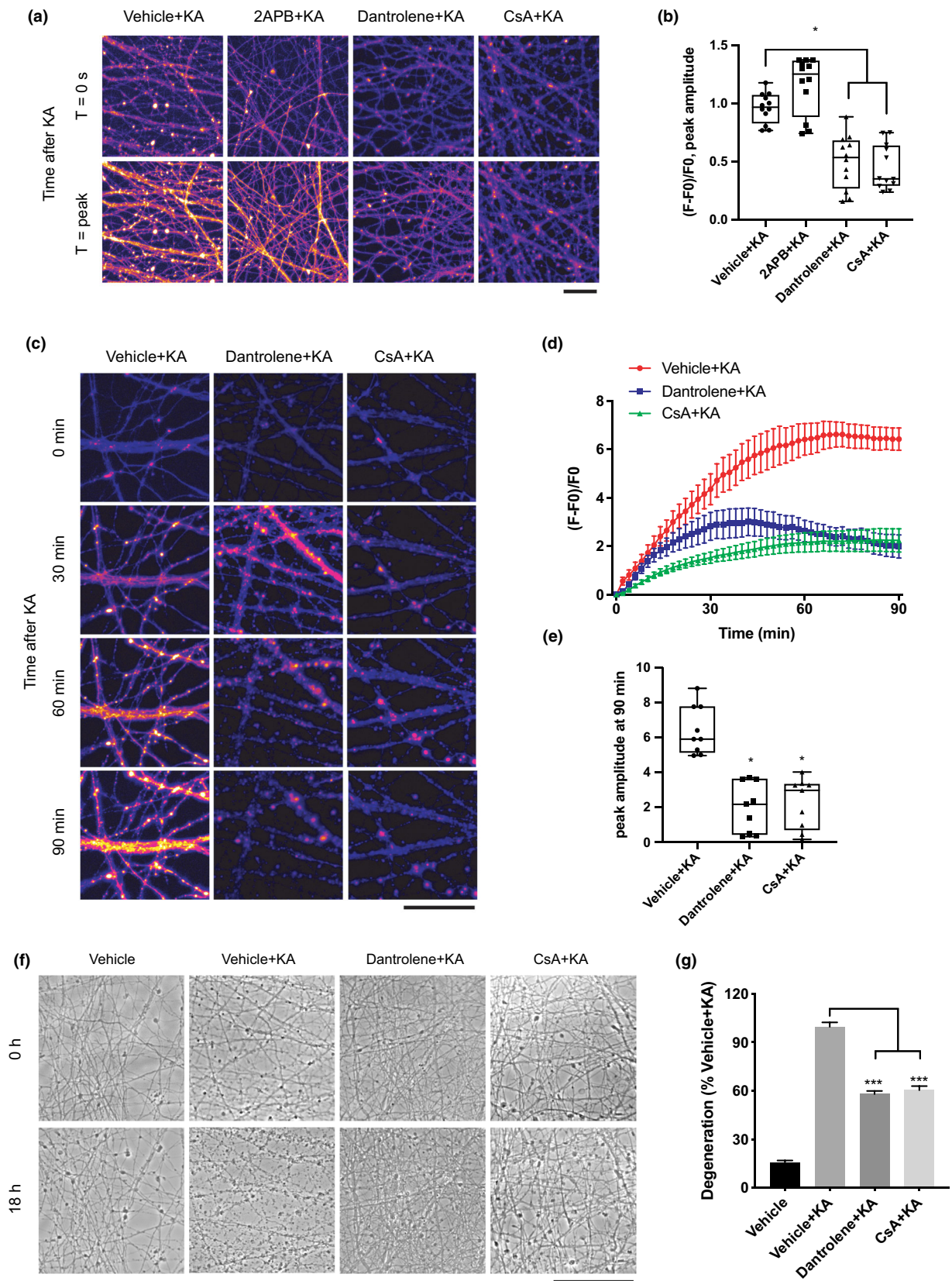
Fig. 5 Inhibition of calcium release from intra-axonal endoplasmic reticulum and mitochondria prevent axonal calcium rise and degeneration. (a) Axons pre-treated with 2APB, Dantrolene and Cyclosporin A before (T = 0 s) and after (T = peak) KA treatment. Scale bar, 50 mm. (b) Quantification of relative calcium peak intensity. Mean ± SEM; n = 12 analysed fields; one-way ANOVA followed by Dunnett's multiple comparisons test; *p < 0.05. (c) The gradual phase of axonal calcium changes with pre-treatment with Dantrolene and Cyclosporin A. Axons of cortical neurons loaded with Fluo-4 before (0 min) and after somal KA treatment (30 min, 60 min, 90 min). Scale bar, 50 mm. (d) Plot of relative calcium intensity changes in the axons after KA treatment for 90 min. Mean ± SEM; n = 9 analysed fields. (e) Quantification of relative calcium intensity at 90 min after KA treatment. Mean ± SEM; n = 9 analysed fields. (f) Phase images of axons acquired before (0 h) and after different dose of KA treatment (18h). Scale bar, 50 mm. (g) Percentage of axon degeneration normalized to Vehicle + KA. Mean ± SEM; n = 40 analysed images; one-way ANOVA followed by Dunnett's multiple comparisons test; ***p < 0.001.

axonal calcium increases have previously been associated with glutamate excitotoxicity, which was shown to induce an initial axonal calcium increase followed by a gradually increase over the next 90 min (Hernandez *et al.,* 2018). In this study, no transient calcium influx was reported, potentially reflecting differences in the age or type of the neurons, which were less mature (7–8 days *in vitro*), potentially prior to action potential induction.

To determine the role of the calcium increases in axon degeneration we utilized the calcium chelators EGTA, to chelate extracellular calcium, and the cell permeant BAPTA-am to chelate intracellular calcium. Both EGTA and BAPTA-am prevented or reduced both the first and second calcium increase within the axonal compartment, however, surprisingly, only BAPTA protected against axonal degeneration. There are a number of potential explanations for the alterations to intracellular calcium in the presence of extracellular EGTA. Firstly, extracellular removal of calcium could deplete the intracellular stores. Stys and Lopachin (1998) demonstrated that exposure of optic nerves to a perfusate lacking calcium reduced total axoplasmic calcium (which included regions of ER) to undetectable levels (Stys and Lopachin, 1998). This suggests a robust exchange of the majority of axonal calcium with the extracellular space in optic fibres, although other fibre tracts may be more resistant to this calcium depletion (Ouardouz *et al.,* 2003). Alternatively, release from intracellular stores could be dependent on an initial extracellular calcium signal through calcium channels in the cell membrane as occurs in calcium induced calcium release. The differential effects of BAPTA and EGTA on axon degeneration, despite both reducing intracellular calcium levels, is less clear but has been previously described (see Matolcsi and Giordano, 2015). For example, Villegas and colleagues demonstrated that mitochondria in sciatic nerve explants were differentially affected by intracellular or extracellular calcium chelation, with mitochondrial swelling inhibited only in the presence of BAPTA-am (Villegas *et al.,* 2014). It is possible that induction of axon degeneration via intracellular calcium release is dependent on subtle calcium changes at specific calcium sensitive nanodomains rather than global intracellular calcium. In this regard, BAPTA is a fast calcium blocker, whereas extracellular EGTA may reduce intracellular calcium, but not in quantities that are sufficient to block these nanodomain effects. BAPTA-am has also been shown to prevent axon degeneration in hippocampal slice cultures exposed to ischemic injury (Tymianski *et al.,* 1994; Abdel-Hamid and Tymianski, 1997).

Calcium influx is sodium channel dependent and involves calcium release from ER and mitochondria

To investigate the source of calcium we used channel blockers and examined the effect on calcium increases in response to kainic acid. Both the initial calcium increase and subsequent gradual calcium rise were blocked by tetrodotoxin, indicating dependence on sodium channels. Sodium channel opening is intimately linked to the action potential and occurs in response to a change in membrane potential. Increases in intracellular sodium could induce increases in axonal calcium via a number of mechanisms. Several studies have implicated voltage gated calcium channels (VGCC) in rapid calcium influx following the action potential, which is dependent on sodium influx, in both peripheral and central neurons, although the type of VGCC involved may vary with cell type. Barzan and colleagues demonstrated calcium transients in peripheral nerves that were dependent on both N and L-type VGCC (Barzan *et al.,* 2016). Furthermore, Jackson *et al* (2001) demonstrated a VGCC dependent calcium increase in sympathetic nerves which was tetrodotoxin dependent. However, this calcium increase did not involve intracellular stores. Callewaert *et al.,* (1996) examined cerebellar Purkinje cells and showed an involvement for P type channels in calcium increases. Sargoy *et al.,* (2014) suggested that L-type channels were involved in retinal ganglion cell calcium influx. Another potential source of sodium induced calcium influx is the sodium/calcium exchanger. This axolemmal ion exchanger usually functions to remove calcium from the cell along the electrochemical gradient of sodium; however, during high intracellular sodium it can operate in reverse (Yu and Choi, 1997). This reverse operation of the sodium/calcium exchanger has been shown to occur in axons under conditions of hypoxia (Stys and Lopachin 1998). It is also possible that intracellular sodium influx can directly stimulate calcium release from intracellular stores. Nikolaeva and colleagues showed that unlike the *in vivo* situation, *in vitro* ischemia to the optic nerve induces a sodium dependent release of calcium from intracellular stores involving both ER (ryanodine and IP3 receptors) and mitochondrial sodium/calcium exchange (Nikolaeva *et al.,* 2005). There is also evidence that ryanodine

receptors can be directly modulated by sodium ions in the sarcoplasmic reticulum of skeletal muscle (Allard and Rougier, 1992; Hu and Kalb 2003).

This study suggests that both action potential-derived calcium transients and axon degeneration-associated secondary calcium flux following excitotoxic injury involves calcium release through the ryanodine receptors as well as stimulating calcium release through the mitochondrial permeability transition pore. Blocking either of these channels provides some protection from axon degeneration. It should be noted however that cyclosporin A, used in this study to block mitochondrial calcium efflux, has known off-target effects such as blocking the activation of calcineurin, implicated in cytoskeletal breakdown (Matsuda and Koyasu, 2000). Previous research has implicated action potential-derived calcium release through ryanodine receptors in axon – oligodendrocyte communication, stimulating glutamate release from the axo-myelinic synapse (Micu *et al.,* 2016). The involvement of MPTP in calcium release following the action potential is less expected, however previous studies have shown that pore opening is not always associated with degenerative pathways and transient opening of the pore has been implicated in somatic reprogramming (Ying *et al.,* 2018) and in acute ischemic preconditioning of cardiomyocytes, which can protect against subsequent sustained ischemia (Hausenloy *et al.,* 2009). The axonal ER and mitochondria are closely coupled (Wu *et al.,* 2017) and previous studies demonstrate the role of ER calcium release in mediating MPTP opening following a variety of insults (Villegas *et al.,* 2014). Together, our data adds to previous data in the field suggesting a complex involvement of intracellular and extracellular calcium in mediating axon degeneration which may depend on the amount/duration of the calcium increase as well as cell type specific involvement of different calcium channels.

The microtubule stabilizing drug taxol acts upstream of the gradual calcium influx to protect against axon fragmentation

Our previous studies have shown that stabilizing microtubules with taxol significantly inhibits axon fragmentation following excitotoxic injury, however the time-course of microtubule dependent processes following the somatodendritic excitotoxic insult are not known. We hypothesized that microtubule alterations would be downstream of intracellular calcium increases. Previous studies have implicated microtubule breakdown in axon degeneration resulting from a variety of insults and these processes have been linked to calcium dependent processes. For example, O'Brien *et al.* (1997) demonstrated that extracted microtubules can undergo spontaneous depolymerization with high calcium level. Furthermore, calcium may activate calpains which can act to degrade microtubule associated proteins (MAPs), which could indirectly cause microtubule breakdown (Zhang *et al.,*

2007; Ferreira and Bigio, 2011). Conversely some studies suggest that microtubule destabilization is upstream of MAP degradation in axons and dendrites (Li *et al.,* 2003; Hoskison and Shuttleworth 2006). In discordance with our hypothesis, stabilization of microtubules with taxol, even at low concentrations, prevented the second, potentially pathological, calcium increase, suggesting that microtubule associated events are upstream of calcium increases. To further investigate the role of taxol in preventing the calcium influx, we examined the effect of 10 ng/mL taxol on microtubule post-translational modifications. Exposure to taxol resulted in decreased microtubule tyrosination and increased acetylation, as has previously been shown in cancer cell lines (Dowdy *et al.,* 2006). One potential explanation for the taxol induced protection is that the secondary calcium increase could be dependent on a microtubule signalling event, which is inhibited by the stabilized microtubules. Microtubules are polymers of alpha and beta tubulin subunits and their highly dynamic properties and role in transport makes them an ideal candidate for the spatial organization of signal transduction molecules within different parts of the cell (Gunderson and Cook 1999). There are a number of ways whereby microtubules could mediate signal transduction, including binding, release or transport of signalling molecules, and these may be affected by alterations in microtubule dynamics, such as stabilization with taxol. Our previous studies and those of others suggest a role for soma- axonal signalling in excitotoxin-induced axon degeneration (King *et al.,* 2013). Alternatively, taxol may result in a more localized effect, such as the uncoupling of ER/mitochondrial nanodomains. Propagation of ER calcium signals to the mitochondria requires close coupling of ER and mitochondria, which are strategically positioned by mitochondrial transport and held in place by tethers (Rizzuto *et al.,* 1998). Previous studies have implicated cytoskeletal modification in calcium release from ER and mitochondria (Wang *et al.,* 2002; Mironov *et al.,* 2005) Thus, taxol may prevent axon degeneration by inhibiting pro-degeneration signalling from the soma or directly altering mitochondrial/ER coupling rather than frank protection of microtubule degradation, which may occur later by a calcium dependent process.

In summary, our data indicate that somatodendritic excitotoxin exposure results in a benign calcium transient in the axon, which at higher concentrations of excitotoxin is likely followed by a soma to axonal signal resulting in a gradual increase in axonal calcium released from ER or mitochondrial stores and resulting in eventual fragmentation of the axon.

References

Abdel-Hamid K. M. and Tymianski M. (1997) Mechanisms and effects of intracellular calcium buffering on neuronal survival in organotypic hippocampal cultures exposed to anoxia/aglycemia or to excitotoxins. *J. Neurosci.* **17**, 3538–3553.

Adalbert R., Morreale G., Paizs M., Conforti L., Walker S. A., Roderick H. L., Bootman M. D., Siklos L. and Coleman M. P. (2012) Intra-axonal calcium changes after axotomy in wild-type and slow Wallerian degeneration axons. *Neuroscience* **225**, 44–54.

Allard B. and Rougier O. (1992) Reappraisal of the role of sodium ions in excitation-contraction coupling in frog twitch muscle. *J. Muscle Res. Cell. Motil.* **13**, 117–125.

Arduino D. M. and Perocchi F. (2018) Pharmacological modulation of mitochondrial calcium homeostasis. *J. Physiol.* **596**, 2717–2733.

Arundine M. and Tymianski M. (2003) Molecular mechanisms of calcium-dependent neurodegeneration in excitotoxicity. *Cell Calcium* **34**, 325–337.

Arundine M. and Tymianski M. (2004) Molecular mechanisms of glutamate-dependent neurodegeneration in ischemia and traumatic brain injury. *Cell. Mol. Life Sci.* **61**, 657–668.

Barzan R., Pfeiffer F. and Kukley M. (2016) N- and L-type voltage-gated calcium channels mediate fast calcium transients in axonal shafts of mouse peripheral nerve. *Front. Cell. Neurosci.* **10**, 135.

Callewaert G., Eilers J. and Konnerth A. (1996) Axonal calcium entry during fast 'sodium' action potentials in rat cerebellar Purkinje neurones. *J. Physiol.* **495**(Pt 3), 641–647.

Cheng C., Fass D. M. and Reynolds I. J. (1999) Emergence of excitotoxicity in cultured forebrain neurons coincides with larger glutamate-stimulated [Ca(2+)] (i) increases and NMDA receptor mRNA levels. *Brain Res.* **849**, 97–108.

Dowdy S. C., Jiang S., Zhou X. C., Hou X., Jin F., Podratz K. C. and Jiang S. W. (2006) Histone deacetylase inhibitors and paclitaxel cause synergistic effects on apoptosis and microtubule stabilization in papillary serous endometrial cancer cells. *Mol. Cancer Ther.* **5**, 2767–2776.

Ferreira A. and Bigio E. H. (2011) Calpain-mediated tau cleavage: a mechanism leading to neurodegeneration shared by multiple tauopathies. *Mol. Med.* **17**, 676–685.

Gundersen G. G. and Cook T. A. (1999) Microtubules and signal transduction. *Curr. Opin. Cell Biol.* **11**, 81–94.

Hausenloy D. J., Ong S. B. and Yellon D. M. (2009) The mitochondrial permeability transition pore as a target for preconditioning and postconditioning. *Basic Res. Cardiol.* **104**, 189–202.

Heath P. R. and Shaw P. J. (2002) Update on the glutamatergic neurotransmitter system and the role of excitotoxicity in amyotrophic lateral sclerosis. *Muscle Nerve* **26**, 438–458.

Hernandez D. E., Salvadores N. A., Moya-Alvarado G., Catalan R. J., Bronfman F. C. and Court F. A. (2018) Axonal degeneration induced by glutamate excitotoxicity is mediated by necroptosis. *J.. Cell Sci.* **131**, jcs214684.

Hilliard M. A. (2009) Axonal degeneration and regeneration: a mechanistic tug-of-war. *J. Neurochem.* **108**, 23–32.

Hosie K. A., King A. E., Blizzard C. A., Vickers J. C. and Dickson T. C. (2012) Chronic excitotoxin-induced axon degeneration in a compartmented neuronal culture model. *ASN Neuro.* **4**, e00076.

Hoskison M. M. and Shuttleworth C. W. (2006) Microtubule disruption, not calpain-dependent loss of MAP2, contributes to enduring NMDA-induced dendritic dysfunction in acute hippocampal slices. *Exp. Neurol.* **202**, 302–312.

Hu P. and Kalb R. G. (2003) BDNF heightens the sensitivity of motor neurons to excitotoxic insults through activation of TrkB. *J. Neurochem.* **84**, 1421–1430.

Jackson V. M., Trout S. J., Brain K. L. and Cunnane T. C. (2001) Characterization of action potential-evoked calcium transients in mouse postganglionic sympathetic axon bundles. *J. Physiol.* **537**(Pt 1), 3–16.

King A. E., Southam K. A., Dittmann J. and Vickers J. C. (2013) Excitotoxin-induced caspase-3 activation and microtubule disintegration in axons is inhibited by taxol. *Acta Neuropathol. Commun.* **1**, 59.

King A. E., Woodhouse A., Kirkcaldie M. T. and Vickers J. C. (2016) Excitotoxicity in ALS: overstimulation, or overreaction? *Exp Neurol* **275**(Pt 1), 162–171.

Knoferle J., Koch J. C., Ostendorf T. *et al.* (2010) Mechanisms of acute axonal degeneration in the optic nerve in vivo. *Proc. Natl Acad. Sci. USA* **107**, 6064–6069.

Li G., Faibushevich A., Turunen B. J., Yoon S. O., Georg G., Michaelis M. L. and Dobrowsky R. T. (2003) Stabilization of the cyclin-dependent kinase 5 activator, p35, by paclitaxel decreases beta-amyloid toxicity in cortical neurons. *J. Neurochem.* **84**, 347–362.

Luarte A., Cornejo V. H., Bertin F., Gallardo J. and Couve A. (2018) The axonal endoplasmic reticulum: one organelle-many functions in development, maintenance, and plasticity. *Dev. Neurobiol.* **78**, 181–208.

Matolcsi M. and Giordano N. (2015) A novel explanation for observed CaMKII dynamics in dendritic spines with added EGTA or BAPTA. *Biophys J* **108**, 975–985.

Matsuda S. and Koyasu S. (2000) Mechanisms of action of cyclosporine. *Immunopharmacology* **47**, 119–125.

Mattson M. P., LaFerla F. M., Chan S. L., Leissring M. A., Shepel P. N. and Geiger J. D. (2000) Calcium signaling in the ER: its role in neuronal plasticity and neurodegenerative disorders. *Trends Neurosci.* **23**, 222–229.

Micu I., Plemel J. R., Lachance C., Proft J., Jansen A. J., Cummins K., van Minnen J. and Stys P. K. (2016) The molecular physiology of the axo-myelinic synapse. *Exp. Neurol.* **276**, 41–50.

Mironov S. L., Ivannikov M. V. and Johansson M. (2005) $[Ca^{2+}]i$ signaling between mitochondria and endoplasmic reticulum in neurons is regulated by microtubules. From mitochondrial permeability transition pore to Ca^{2+}-induced Ca^{2+} release. *J. Biol. Chem.* **280**, 715–721.

Mishra B., Carson R., Hume R. I. and Collins C. A. (2013) Sodium and potassium currents influence Wallerian degeneration of injured Drosophila axons. *J. Neurosci.* **33**, 18728–18739.

Nikolaeva M. A., Mukherjee B. and Stys P. K. (2005) Na^+-dependent sources of intra-axonal Ca^{2+} release in rat optic nerve during in vitro chemical ischemia. *J. Neurosci.* **25**, 9960–9967.

O'Brien E. T., Salmon E. D. and Erickson H. P. (1997) How calcium causes microtubule depolymerization. *Cell. Motil. Cytoskeleton* **36**, 125–135.

Ouardouz M., Nikolaeva M. A., Coderre E., Zamponi G. W., McRory J. E., Trapp B. D., Yin X., Wang W., Woulfe J. and Stys P. K. (2003) Depolarization-induced Ca^{2+} release in ischemic spinal cord white matter involves L-type Ca^{2+} channel activation of ryanodine receptors. *Neuron* **40**, 53–63.

Pellegrini-Giampietro D. E., Gorter J. A., Bennett M. V. and Zukin R. S. (1997) The GluR2 (GluR-B) hypothesis: Ca(2+)-permeable AMPA receptors in neurological disorders. *Trends Neurosci.* **20**, 464–470.

Rizzuto R., Pinton P., Carrington W., Fay F. S., Fogarty K. E., Lifshitz L. M., Tuft R. A. and Pozzan T. (1998) Close contacts with the endoplasmic reticulum as determinants of mitochondrial Ca^{2+} responses. *Science* **280**, 1763–1766.

Ruiz A., Matute C. and Alberdi E. (2009) Endoplasmic reticulum Ca(2+) release through ryanodine and IP(3) receptors contributes to neuronal excitotoxicity. *Cell Calcium* **46**, 273–281.

Sargoy A., Sun X., Barnes S. and Brecha N. C. (2014) Differential calcium signaling mediated by voltage-gated calcium channels in rat retinal ganglion cells and their unmyelinated axons. *PLoS ONE* **9**, e84507.

Staal J. A., Dickson T. C., Gasperini R., Liu Y., Foa L. and Vickers J. C. (2010) Initial calcium release from intracellular stores followed by calcium dysregulation is linked to secondary axotomy following transient axonal stretch injury. *J. Neurochem.* **112**, 1147–1155.

Stys P. K. and Lopachin R. M. (1998) Mechanisms of calcium and sodium fluxes in anoxic myelinated central nervous system axons. *Neuroscience* **82**, 21–32.

Szydlowska K. and Tymianski M. (2010) Calcium, ischemia and excitotoxicity. *Cell Calcium* **47**, 122–129.

Tymianski M. and Tator C. H. (1996) Normal and abnormal calcium homeostasis in neurons: a basis for the pathophysiology of traumatic and ischemic central nervous system injury. *Neurosurgery* **38**, 1176–1195.

Tymianski M., Spigelman I., Zhang L., Carlen P. L., Tator C. H., Charlton M. P. and Wallace M. C. (1994) Mechanism of action and persistence of neuroprotection by cell-permeant Ca^{2+} chelators. *J. Cereb. Blood Flow Metab.* **14**, 911–923.

Vargas M. E., Yamagishi Y., Tessier-Lavigne M. and Sagasti A. (2015) Live imaging of calcium dynamics during axon degeneration reveals two functionally distinct phases of calcium influx. *J. Neurosci.* **35**, 15026–15038.

Vickers J. C., King A. E., Woodhouse A. *et al.* (2009) Axonopathy and cytoskeletal disruption in degenerative diseases of the central nervous system. *Brain Res. Bull.* **80**, 217–223.

Villegas R., Martinez N. W., Lillo J., Pihan P., Hernandez D., Twiss J. L. and Court F. A. (2014) Calcium release from intra-axonal endoplasmic reticulum leads to axon degeneration through mitochondrial dysfunction. *J. Neurosci.* **34**, 7179–7189.

Wang R. and Reddy P. H. (2017) Role of glutamate and NMDA receptors in Alzheimer's disease. *J. Alzheimers Dis.* **57**, 1041–1048.

Wang Y., Mattson M. P. and Furukawa K. (2002) Endoplasmic reticulum calcium release is modulated by actin polymerization. *J. Neurochem.* **82**, 945–952.

Wang J. T., Medress Z. A. and Barres B. A. (2012) Axon degeneration: molecular mechanisms of a self-destruction pathway. *J. Cell Biol.* **196**, 7–18.

Wu Y., Whiteus C., Xu C. S., Hayworth K. J., Weinberg R. J., Hess H. F. and De Camilli P. (2017) Contacts between the endoplasmic reticulum and other membranes in neurons. *Proc. Natl Acad. Sci. USA* **114**, E4859–e4867.

Yang J., Weimer R. M., Kallop D., Olsen O., Wu Z., Renier N., Uryu K. and Tessier-Lavigne M. (2013) Regulation of axon degeneration after injury and in development by the endogenous calpain inhibitor calpastatin. *Neuron* **80**, 1175–1189.

Yawo H. and Kuno M. (1985) Calcium dependence of membrane sealing at the cut end of the cockroach giant axon. *J. Neurosci.* **5**, 1626–1632.

Ying Z., Xiang G., Zheng L. *et al.* (2018) Short-term mitochondrial permeability transition pore opening modulates histone lysine methylation at the early phase of somatic cell reprogramming. *Cell Metab.* **29**, 502.

Yu S. P. and Choi D. W. (1997) Na(+)-Ca^{2+} exchange currents in cortical neurons: concomitant forward and reverse operation and effect of glutamate. *Eur. J. Neurosci.* **9**, 1273–1281.

Zhang Z., Ottens A. K., Sadasivan S., Kobeissy F. H., Fang T., Hayes R. L. and Wang K. K. (2007) Calpain-mediated collapsin response mediator protein-1, -2, and -4 proteolysis after neurotoxic and traumatic brain injury. *J. Neurotrauma* **24**, 460–472.